Polymer 43 (2002) 2085–2088

polymer

www.elsevier.com/locate/polymer

Nanoscale artifacts in RuO_4-stained poly(styrene)

T.M. Chou, P. Prayoonthong, A. Aitouchen, M. Libera*

Department of Chemical, Biochemical, and Materials Engineering, Stevens Institute of Technology, Hoboken, NJ 07030, USA

Received 26 September 2001; received in revised form 8 November 2001; accepted 13 November 2001

Abstract

This research studies the effects of RuO_4 exposure on various samples of poly(styrene) (PS). Transmission electron energy-loss spectroscopy (EELS) shows a decrease in the 7 eV $\pi-\pi*$ transition characteristic of aromatic rings in PS indicating that RuO_4 covalently alters aromatic character. Imaging and selected-area electron diffraction show that a layer of RuO_2 solid forms on the surface of bulk PS specimens exposed to RuO_4. High-resolution TEM imaging (HREM) shows that RuO_2 nanocrystals consistently condense on specimen surfaces, independent of the chemical nature of the specimen below. These nanocrystals modulate contrast at length scales on the order of 2–5 nm in TEM images and limit resolution at nanometer length scales. © 2002 Elsevier Science Ltd. All rights reserved.

Keywords: Ruthenium tetroxide; Electron microscopy; Poly(styrene)

The contrast observed in transmission electron microscope (TEM) images between different phases in a multiphase polymeric material is usually poor, because most organic polymers have similar compositions and densities. Different polymer phases thus produce comparable levels of elastic electron scattering. Differential heavy-element stains are consequently used to preferentially decorate one phase. Heavy-element stains enhance high-angle Rutherford scattering, which scales with atomic number (Z) as $\sim Z^{4/3}$ for a screened atomic potential. Image contrast, $C = \Delta I/I$ where I is the image intensity characteristic of the background and ΔI represents intensity deviations from that background, can then be generated by using an objective aperture to block electrons scattered to high angles from stained regions of material. Stained regions then have dark contrast, and unstained or less-stained regions have light contrast.

The particular choice of which stain to use in a given polymer system is guided largely by empirical success. OsO_4 is perhaps among the best known staining agents and is routinely used to decorate unsaturation such as that characteristic of diene rubbers [1,2]. OsO_4 is believed to act as a covalent crosslinker between unsaturated carbon double bonds [3] thus affecting the specimen's mechanical properties as well as its electron-scattering behavior. Other stains such as uranyl acetate and phosphotungstaic acid are believed to accumulate in regions of high local free volume. Protocols for use and typical applications of these and a number of other stains are discussed by Sawyer and Grubb [4].

Ruthenium tetroxide was introduced as a differential stain in 1983 by Trent et al. [5]. Techniques based on Ru-based staining continue to be developed [6,7]. It is principally used to differentially label aromatic moieties from aliphatic ones. It can also preferentially localize in regions of low density. For the most part, imaging applications that have used RuO_4 as well as most other heavy-element stains have been performed at low to intermediate magnifications on the order of 1000–40,000 ×. These magnifications are sufficient to resolve the mesoscale structure of interest, for example, in polymer blends and microphase-separated block copolymers.

Here we explore the effectiveness of RuO_4 as a label of polymer morphology at nanometer scale resolution. This length scale is relevant to studies of polymer interfaces as well as to studies of globular and dendritic polymers (e.g. dendrimers, hyperbranched polymers, arborescent polymers, microgels). Despite the fact that RuO_4 exposure covalently opens aromatic rings in poly(styrene) (PS), RuO_2 nanocrystals, approximately 2–5 nm in diameter, deposit on sample surfaces and lead to imaging artifacts at high resolution. This finding suggests that alternate electron-optical imaging methods, such as those based on spatially resolved electron energy-loss spectroscopy, which do not rely on the introduction of stains, may be more appropriate for high spatial resolution investigations.

The materials studied in this work were: (i) bulk PS (Scientific Polymer Products; $M_w = 190{,}000$ g/mole); and

---

* Corresponding author. Tel.: +1-201-216-5259, fax: +1-201-216-8306.
E-mail address: mlibera@stevens-tech.edu (M. Libera).

0032-3861/02/$ - see front matter © 2002 Elsevier Science Ltd. All rights reserved.
PII: S0032-3861(01)00767-4

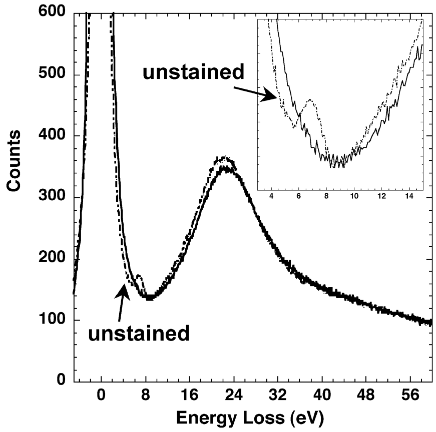

Fig. 1. Electron energy-loss spectra from unstained (dashed) and stained (solid) poly(styrene) showing that the 7 eV peak intensity characteristic of the aromatic $\pi-\pi*$ transition decreases with exposure to RuO_4 vapor.

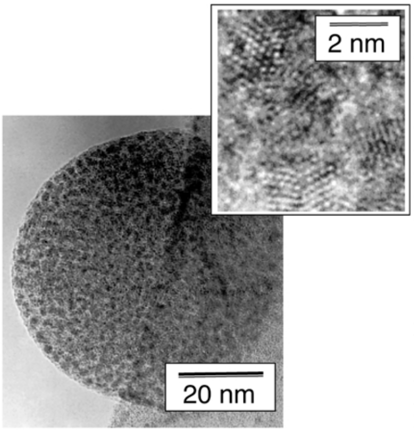

Fig. 2. High-resolution TEM image of nanoscale crystallites on a poly-(styrene) latex sphere after exposure to RuO_4 vapor.

(ii) PS latex spheres ~80–100 nm in diameter (courtesy of Dr V. Demonie, Lehigh University Emulsion Polymers Institute). Electron-transparent sections (~80 nm thick) were cut at room temperature from bulk specimens (i) using a Riechart Ultracut E cryomicrotome and collected on copper TEM grids. Latex specimens (ii) were dispersed on a holey-carbon TEM support grid by placing a drop of dilute aqueous solution on the grid and allowing the water to evaporate. Heavy-element staining was performed by exposing thin specimens to vapor from a room-temperature solution of 0.5 wt% RuO_4 in water (Electron Microscopy Sciences, Fort Washington, PA) for either: (a) ~30 min; or (b) 3 days. In the case of the microtomed sections (i), the staining procedure was applied after cutting the thin section rather than to a bulk block face prior to cutting.

The specimens were studied by bright-field TEM imaging, high-resolution (HREM) TEM imaging, and electron energy-loss spectroscopy (EELS). Imaging was done using a Philips CM30 SuperTwin TEM at 300 keV with a point resolution of 0.19 nm. Energy-loss spectroscopy was done using a field-emission 200 keV Philips CM20 TEM/STEM with a Gatan 666 parallel electron energy-loss (PEELS) spectrometer

The chemical effect on PS of RuO_4 stain is demonstrated by Fig. 1. This shows the low loss part of energy-loss spectra collected from a PS, specimen (i) subjected to staining protocol (a), both before and after exposure to the stain. The unstained PS displays a peak at approximately 7 eV energy loss. This is a well known spectroscopic feature [8–11] associated with a $\pi-\pi*$ bonding-antibonding excitation within the phenyl ring. This peak disappears after staining indicating that the stain has covalently reacted with aromatic rings in the specimen. No attempt was made here to establish the fraction of aromaticity affected by the stain. The slight shift in the plasmon ($\sigma-\sigma*$) peak circa 23 eV energy loss is presumably due to the change in valence–electron concentration introduced by the oxide stain. As in the case of OsO_4-stained dienes, RuO_4-stained aromatics appear more brittle than when unstained. Together these observations suggest that RuO_4 both opens aromatic rings and serves as a crosslinker between adjacent aromatic structures similar to the manner in which OsO_4 is believed to crosslink unsaturated diene rubbers [4].

The fact that nanocrystals form on the specimen during the staining process is illustrated by Fig. 2. The specimen is a PS latex sphere protruding into the vacuum and supported by the carbon film in a holey-carbon TEM grid. Fig. 2 shows an HREM image of the entire latex sphere. Mottled contrast across the specimen is evident. At higher magnification, the high-resolution image in the inset to Fig. 2 shows that the mottled contrast is due to a distribution of crystalline particles randomly oriented with respect to the incident electron beam. These crystals are equiaxed with sizes of order 2–5 nm.

Despite the fact that staining by the covalent reaction between RuO_4 and a specimen depends strongly on the spatial distribution of aromatic moieties, the RuO_2 nanocrystals appear able to deposit on almost any surface. This has been most convincingly demonstrated by observing RuO_2 nanocrystals, identical to those on the PS latex sphere in Fig. 2, deposited uniformly on a plain carbon film when subjected to a typical RuO_4-staining exposure (i.e. staining protocol (a)). Indeed, nanocrystals have been observed with no obvious preference in spatial distribution using a variety of different polymer specimens including styrene–diene block copolymers as well as PS–poly(2-vinyl pyridine) blends among others. We have evidence that exposure to OsO_4 produces similar surface nanocrystals.

To resolve whether the crystalline nanoparticles reside on the surface of the polymer specimen or possibly within its bulk, a cross-sectional specimen was cut from a bulk sample of pure PS after a 3-day (staining protocol (b)) exposure to RuO_4 vapor. A bright-field TEM image of one such specimen is presented in Fig. 3a. There is a layer with dark contrast at the free surface of the specimen. The fact that this layer is crystalline is confirmed by the selected-area electron diffraction pattern presented in Fig. 3b. The grains

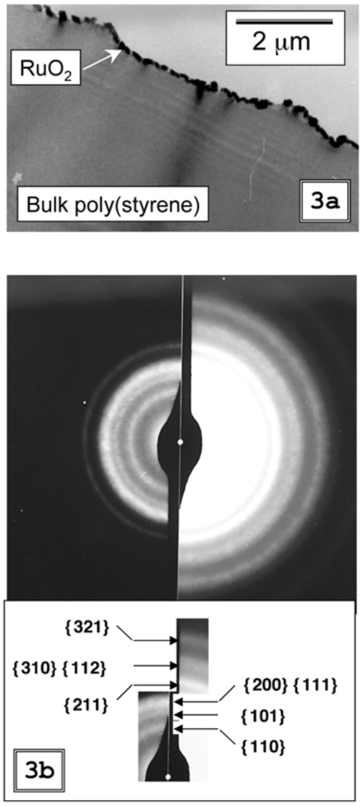

Fig. 3. (a) Bright-field TEM image of a bulk specimen of poly(styrene) viewed in cross-section. The specimen was exposed to RuO_4 vapor prior to sectioning. (b) Selected-area electron diffraction pattern with reflections indicating that the dark-contrast surface layer is RuO_2.

within the surface layer have random orientations as manifested by the continuous Debye–Scherrer rings in this pattern. Each ring is relatively broad, consistent with the real-space observation (Fig. 2) that the grains within the film are extremely small. The magnitudes of the scattering vectors associated with each of the principal diffracted rings in the pattern of Fig. 3b were measured, and ratios of these agree very well with ratios determined from standard d-spacings characteristic of RuO_2 given in the JCPDS database [12].

Surface nanocrystals serve principally to reduce image contrast in standard low and intermediate-resolution amplitude-contrast imaging. For the most part, this should be a relatively minor effect and would go largely unnoticed. Assuming a typical pixel size of 25 μm either on a piece of recording film or on a digital camera, a magnification of approximately 40,000 × would be needed to resolve a 3 nm diameter particle using 5 pixels. At magnifications 5–10 × less than this, any surface nanoparticles would simply contribute to an average scattering applied uniformly across an entire specimen. Except in a few exceptional cases, such a uniform decrease in contrast would be superimposed on the very strong contrast due to the clear preferential covalent staining ability of RuO_4 on aromatic moieties.

Morphological studies that demand higher resolution will be more sensitive to the presence of surface nanocrystals. At magnifications greater than about 40,000 ×, individual nanocrystals can be resolved. In a high-magnification image, nanocrystals would lead to speckle in the contrast. In a high-resolution profile of scattered intensity across an interface, they would lead to noise. The many developments in innovative polymer synthesis, together with challenging ultrastructure questions in the biological community, increasingly require morphological information at length scales ranging from ~1 to ~20 nm. The presence of surface nanocrystals may substantially compromise the quality and usefulness of data collected by high-angle elastic electron scattering from RuO_4-stained specimens.

Surface nanocrystal artifacts can be avoided, if exposure to RuO_4 can be achieved before a polymeric specimen is in thin-film electron–transparent form. In studies of bulk samples, long-time exposure to RuO_4 can be done to stain the sample to a substantial depth below the surface. Imaging experiments by scanning electron microscopy (SEM) of heavily-stained bulk PS and PS–PVP blends done as part of the present work indicate that the RuO_2 surface layer prevents useful imaging of the underlying polymer morphology. RuO_2 is a fairly good electrical conductor [13,14], and SEM examination of heavily stained bulk specimens does not suffer from electrical charging problems typical of most bulk polymeric specimens. A surface oxide layer on a bulk specimen can be removed during microtomy. In Fig. 3a, for example, the oxide is localized in a clearly identifiable layer at the specimen surface. The underlying PS phase contains covalently bound RuO_4, and the top and bottom surfaces of the sectioned TEM specimen do not have nanocrystals. However, in the case of solution-cast thin films as well as of individual globular polymers such as dendrimers, hyperbranched polymers, arborescent polymers, and microemulsions, the specimen geometry mandates that the surfaces exposed to RuO_4 be included in the imaging experiment. For high-resolution studies in these cases, alternate stains or mechanisms for TEM image contrast, such as chemical or compositional imaging using some form of energy filtering, must be explored.

In conclusion, this research used PS as a model material to study the effects of exposure to RuO_4 vapor under conditions typical of how one would stain an aromatic material for study in the transmission electron microscope. Electron energy-loss spectroscopy shows that reaction with RuO_4 breaks the π-bond associated with aromatic rings in PS, presumably due to a covalent crosslinking reaction. In addition to the penetration of ruthenium oxide into the bulk of the polymer, RuO_2 nanocrystals form on the polymer surface. These surface nanoparticles have characteristic dimensions on the order of 2–5 nm. They can introduce artifactual structure when studying morphological features such as interfaces and globular polymer nanostructures at high resolution. Under conditions of heavy staining, a continuous film of electrically-conductive RuO_2 forms. RuO_2 surface films reduce the overall contrast that can be obtained in both transmission and scanning electron imaging.

Acknowledgements

This work was supported by the Army Research Office (grant #DAAG55-97-1-0137) and uses instrumentation jointly funded by the National Science Foundation and the New Jersey Commission on Science and Technology.

References

[1] Andrews E. Journal of Polymer Science 1965;3:353.

[2] Kato K. Polymer Engineering and Science 1967;1:38–39.

[3] Ribbe A, Bodycomb J, Hashimoto T. Macromolecules 1999;32(9):3154–6.

[4] Sawyer LC, Grubb DT. Polymer microscopy. 2nd ed. London: Chapman and Hall, 1996.

[5] Trent J, Scheinbeim J, Couchman P. Macromolecules 1983;16:589–98.

[6] Huong D, Dreschler M, Cantow H-J, Moller M. Macromolecules 1993;26:864–6.

[7] Li J, Ness J, Cheung W. Journal of Applied Polymer Science 1996;59:1733–40.

[8] Hunt JA, Disko MM, Behal SK, Leapman RD. Ultramicroscopy 1995;58:55–64.

[9] Ritsko JJ, Bigelow RW. Journal of Chemical Physics 1978;69(9):4162–70.

[10] Siangchaew K, Libera M. Microscopy and Microanalysis 1997;3:530–9.

[11] Swanson N, Powell CJ. Journal of Chemical Physics 1963;39:630–3.

[12] JCPDS, Joint Committee on Powder Diffraction Standards (JCPDS), PDF#43-1027, 1601 Park Lane, Swarthmore, Pa. 19081.

[13] Bai G, Wang A, Foster C, Vetrone J. Thin Solid Films 1997;310:75–80.

[14] Tanaka M, Ami M. Journal of the American Ceramic Society 81(10):2513–6.